



Comparative pharmacology of recombinant human M₃ and M₅ muscarinic receptors expressed in CHO-K1 cells

*¹Nikki Watson, ¹Donald V. Daniels, ¹Anthony P.D.W. Ford, ¹Richard M. Eglen & ¹Sharath S. Hegde

¹Urogenital Pharmacology, Center for Biological Research, Neurobiology Unit, Roche Bioscience, 3401 Hillview Avenue, Palo Alto, California, CA 94304, U.S.A.

1 Affinity estimates were obtained for several muscarinic antagonists against carbachol-stimulated [³H]-inositol phosphates accumulation in Chinese hamster ovary (CHO-K1) cells stably expressing either human muscarinic M₃ or M₅ receptor subtypes. The rationale for these studies was to generate a functional antagonist affinity profile for the M₅ receptor subtype and compare this with that of the M₃ receptor, in order to identify compounds which discriminate between these two subtypes.

2 The rank order of antagonist apparent affinities (pK_B) at the muscarinic M₅ receptor was atropine (8.7) ≥ tolterodine (8.6) = 4-diphenylacetoxy-N-methylpiperidine (4-DAMP, 8.6) > darifenacin (7.7) ≥ zamifenacin (7.6) > oxybutynin (6.6) = para-fluorohexahydrosiladifenidol (p-F-HHSiD, 6.6) > pirenzepine (6.4) ≥ methoctramine (6.3) = himbacine (6.3) > AQ-RA 741 (6.1).

3 Antagonist apparent affinities for both receptor subtypes compare well with published binding affinity estimates. No antagonist displayed greater selectivity for the muscarinic M₅ subtype over the M₃ subtype, but himbacine, AQ-RA 741, p-F-HHSiD, darifenacin and oxybutynin displayed between 9- and 60 fold greater selectivity for the muscarinic M₃ over the M₅ subtype.

4 This study highlights the similarity in pharmacological profiles of M₃ and M₅ receptor subtypes and identifies five antagonists that may represent useful tools for discriminating between these two subtypes. Collectively, these data show that in the absence of a high affinity M₅ selective antagonist, affinity data for a large range of antagonists is critical to define operationally the M₅ receptor subtype.

Keywords: Muscarinic M₃ and M₅ receptors; inositol phosphates accumulation; CHO-K1 cells; muscarinic antagonists

Abbreviations: A, agonist; [A]₅₀, concentration of agonist causing 50% effect; B, antagonist; [B]₅₀, concentration of antagonist causing 50% effect; CHO-K1, Chinese hamster ovary cells; 4-DAMP, 4-diphenylacetoxy-N-methylpiperidine; DPM, disintegrations per minute; EC₅₀, concentration producing half maximal effect; EDTA, ethylenediaminetetraacetic acid; E_m, maximal effect; InsPs, inositol phosphates; nH, Hill slope; PBS, phosphate buffered saline; pEC₅₀, potency; p-F-HHSiD, para-fluorohexahydrosiladifenidol; pK_B, antagonist apparent affinity estimate; r, correlation coefficient; SSQ, sum of squares of differences ($\sum(x-y)^2$)

Introduction

The existence of five subtypes of the muscarinic receptor is now established and identification of pharmacological correlates for all but the fifth gene product has been achieved. However, despite the lack of an endogenous correlate for this subtype it has been given the upper case nomenclature (M₅ rather than m5) based on data generated in cultured cell lines (see Caulfield & Birdsall, 1998 for review). The inability to identify clearly an endogenous population of M₅ receptors and to ascribe a function to this gene product stems from its restricted anatomical expression and the lack of selective antagonists for this subtype. The muscarinic M₅ receptor is 532 amino acids long and, like the M₃ receptor possesses a large third intracellular loop (Reever *et al.*, 1997). The muscarinic M₅ subtype also exhibits an antagonist affinity profile similar to that of the M₃ subtype, which has complicated the identification of a functional correlate. Moreover, it is possible that an endogenous M₅ population has been observed but incorrectly classified as an M₃ receptor. Several groups (Buckley *et al.*, 1989; Dörje *et al.*, 1991; Bolden *et al.*, 1992; Lazareno & Birdsall, 1993) have reported antagonist affinity profiles at the M₅ receptor subtype derived from binding studies using membrane homogenates of cells expressing the

recombinant cloned receptor, including our own (Eglen *et al.*, 1997). However, comparable data have not been reported for functional responses mediated *via* M₅ receptors.

The aim of the present studies was to establish antagonist affinity estimates for a range of muscarinic receptor antagonists against carbachol-stimulated [³H]-inositol phosphates accumulation in CHO-K1 cells stably expressing either human recombinant muscarinic M₃ or M₅ receptors. Having established these functional antagonist affinity estimates these values were compared with published binding affinity estimates for these compounds to determine concordance with the literature, but were also compared with each other, in order to identify compounds which discriminate between these two receptor subtypes. In this way compounds would be identified that could represent useful tools in discriminating between these two receptor subtypes.

Preliminary accounts of this work have been presented to the British Pharmacology Society (Eglen *et al.*, 1997; Watson *et al.*, 1998).

Methods

Tissue culture

Chinese hamster ovary cells (CHO-K1) stably expressing human recombinant muscarinic M₃ and M₅ receptor protein

*Author for correspondence; E-mail: nikki.watson@roche.com

were cultured to confluence in tissue culture flasks (T-162). Culture flasks containing Ham's F-12 nutrient medium supplemented with 10% foetal bovine serum, geneticin (150 µg ml⁻¹) and penicillin/streptomycin (30 µg ml⁻¹, 30 µg ml⁻¹) at 37°C in 7% CO₂. Cells were used at between passages 8 and 20 for both systems.

Inositol phosphates accumulation

The method used was a modification of the procedure reported by Brown and colleagues (1984). Briefly, transfected cells were grown to 80% confluence and washed twice in phosphate buffered saline (PBS) prior to incubating overnight in 15 ml inositol-free Ham's F-12 containing 10% dialyzed foetal bovine serum and 25 µCi [³H]-*myo*-inositol. Following incorporation, the medium was aspirated and the cells washed with PBS to remove unincorporated [³H]-*myo*-inositol. PBS containing ethylene diamine tetraacetic acid (EDTA, 30 µM for 5–10 min at 37°C) was used to dissociate cells from the flask. The cell suspension was centrifuged for 5 min at 500 × g at 37°C and washed three times in PBS. The cells were resuspended in inositol-free Ham's to 10⁶ to 3 × 10⁶ cells ml⁻¹ M₃ and M₅, respectively. Reactions were performed in triplicate in tubes containing 300 µl final reaction volume. Cell suspension (240 µl) was added to 30 µl antagonist or vehicle for pre-equilibration at 37°C for 20 min. The reaction was initiated with the addition of 30 µl agonist or vehicle, containing LiCl (final concentration 10 mM). Tubes were then gently mixed and placed in a 37°C bath for 5 or 10 min for M₅ and M₃ cells, respectively. Reactions were terminated by the addition of 50 µl ice-cold perchloric acid (20%). Tubes were allowed to sit in an ice-water bath for 20 min and samples were then neutralized with 160 µl KOH (1 M) and vortex-mixed. Samples were then diluted with the addition of 2 ml Tris-HCl (50 mM, pH 7.5) and decanted onto disposable columns containing 1 ml Dowex AG 1 × 8, chloride form (1 : 1, w v⁻¹) slurry which had been washed with 5 ml distilled H₂O. Columns were then washed with 20 ml distilled H₂O and the

eluate discarded. [³H]-Inositol phosphates (InsPs) were eluted with 3 ml HCl (1 M) into scintillation vials containing 15 ml Ready-Safe liquid scintillation cocktail.

Data analysis

Accumulated [³H]-InsPs were measured by liquid scintillation spectroscopy using a Packard 1900TR (using standard [³H]-window settings) and expressed as disintegration per minute (DPM). DPM values were imported into Microsoft Excel for determination of mean and standard deviation values for each triplicate. Iterative, nonlinear curve-fitting methods using Kaleidagraph software were used to fit data to the general logistic functions: $\text{Effect} = \text{basal} + E_m \cdot A^{nH} / (A^{nH} + [A]_{50}^{nH})$ for

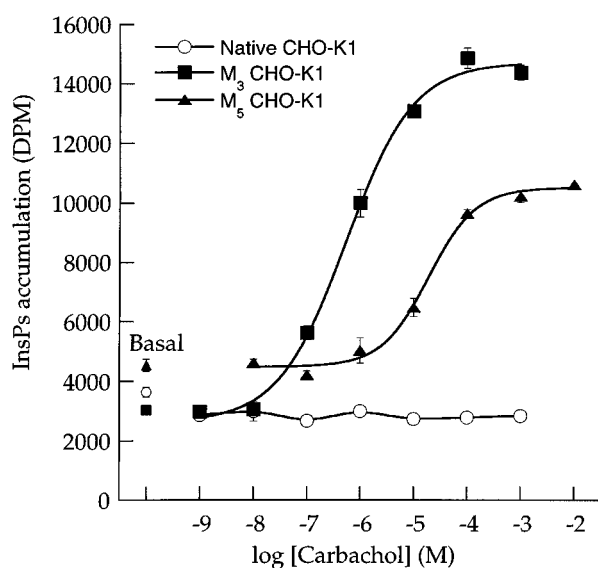


Figure 1 Carbachol-stimulated [³H]-InsPs accumulation in native CHO-K1 cells and those expressing human recombinant muscarinic M₃ and M₅ receptors. Data shown are from single experiments performed in triplicate. Within-experiment means and standard deviations are shown.

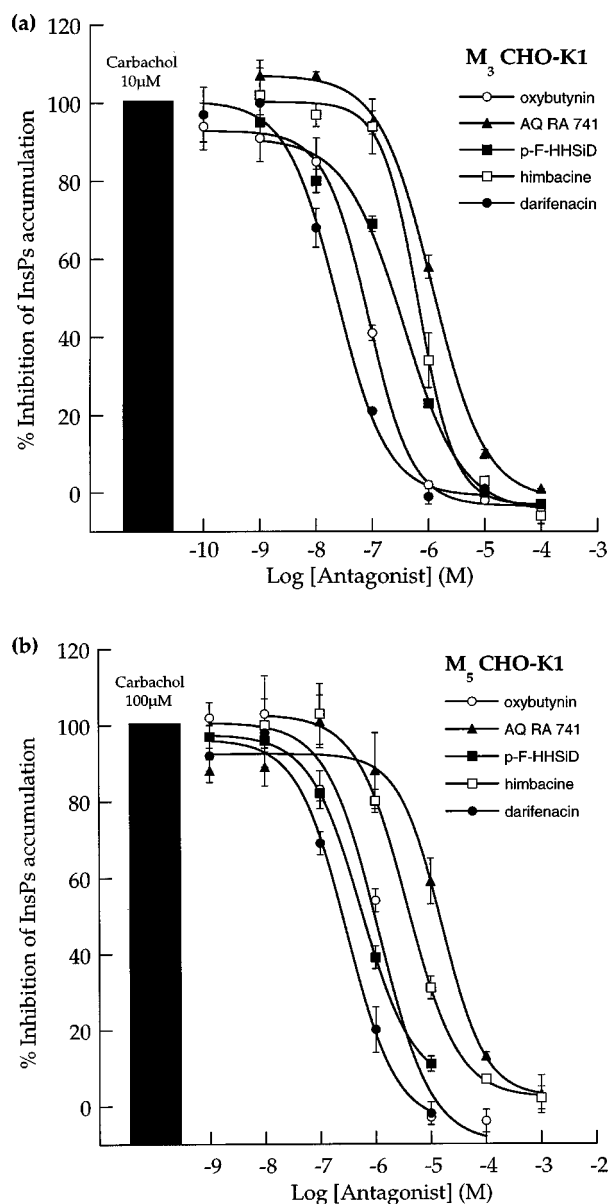


Figure 2 Inhibition of carbachol-stimulated [³H]-InsPs accumulation in CHO-K1 cells expressing human recombinant muscarinic M₃ (a) and M₅ (b) receptors. Responses were obtained to a single concentration of carbachol alone and after equilibration with increasing concentrations of antagonist (20 min antagonist equilibration, 10 and 5 min agonist stimulation for M₃ and M₅, respectively). Data are from representative experiments performed in triplicate. Within-experiment means and standard deviations are shown.

agonist stimulation curves and, $\text{effect} = \text{basal} + E_m - (E_m \cdot B^{nH} / (B^{nH} + [B]_{50}^{nH}))$ for antagonist inhibition curves, in order to establish agonist EC₅₀ ([A]₅₀) antagonist EC₅₀ ([B]₅₀), maxima (E_m) and Hill slopes (nH) for each curve. EC₅₀ being the concentration of agonist or antagonist producing a half maximal effect. Apparent affinity values of antagonists (pK_B) were calculated using the Leff & Dougall (1993) modification of the Cheng-Prusoff equation (Cheng & Prusoff, 1973) such that $K_B = [B]_{50} / (([A] / [A]_{50}^{nH})^{1/nH} - 1)$. All values quoted are the mean \pm s.e.mean of 3–4 individual experiments each performed in triplicate, unless otherwise stated.

Materials

Ham's F-12 nutrient medium, phosphate buffered saline, geneticin (G418), foetal bovine serum (qualified and dialyzed), penicillin/streptomycin and versene (EDTA) were obtained from Gibco (Gaithersburg, MD, U.S.A.). *Myo*-[2-³H] inositol (10–20 Ci mmol⁻¹) was obtained from Amersham (Arlington Heights, IL, U.S.A.). Disposable plastic columns (CC-09-M) were obtained from E&K Scientific Products (Saratoga, CA, U.S.A.). Carbachol was obtained from Research Biochemicals International (Natick, MA, U.S.A.). Bulk chemicals and reagents were obtained from Sigma Chemical (St. Louis, MO, U.S.A.). All other compounds were synthesized by Medicinal Chemistry, Neurobiology Unit, Roche Bioscience (Palo Alto, CA, U.S.A.). Chinese hamster ovary cells (CHO-K1)

expressing human muscarinic M₃ and M₅ receptor proteins were kindly prepared by Mr Steve Delgado in the laboratory of Dr David Chang, Center for Biological Research, Roche Bioscience (Palo Alto). Kaleidagraph Software was purchased from Synergy Software (Reading, PA, U.S.A.). Ready-Safe liquid scintillation cocktail was purchased from Baxter Scientific (McGraw Park, IL, U.S.A.). Himbacine was kindly provided by Professor Taylor (University of New South Wales, Australia). AQ-RA 741 was a generous gift from Boehringer Ingelheim Pharmaceuticals Inc., U.S.A. Darifenacin and zamifenacin were generously provided by Pfizer Central Research (Kent, England). All drugs were prepared using distilled water, with the exception of darifenacin and zamifenacin, these were prepared in DMSO (10% in 10⁻² M stock solution). All dilutions were prepared using distilled water.

Results

Carbachol-stimulated [³H]-InsPs accumulation

Preliminary studies investigating the time-course of carbachol-stimulated [³H]-InsPs accumulation indicated that a 10 min and 5 min agonist exposure time was within the linear portion of the [³H]-InsPs accumulation curve in the CHO-K1 M₃ and M₅ receptor systems, respectively (data not shown). These,

Table 1 Antagonist affinity estimates derived from InsPs studies compared with Tris-Krebs binding data at muscarinic M₃ receptors

Antagonist	*pK _i	pK _B	s.e.mean	Hill slope	s.e.mean	n
Atropine	9.5	8.6	0.1	1.1	0.1	4
Pirenzepine	6.8	6.4	0.1	1.0	0.1	4
Methoctramine	6.1	6.8	0.1	1.1	0.3	3
AQ-RA 741	7.2	7.1	0.1	0.9	0.1	3
Himbacine	6.9	7.2	0.1	1.1	0.1	3
4-DAMP	9.3	8.8	0.1	1.1	0.1	4
p-F-HHSiD	7.5	7.6	0.1	1.0	0.2	3
Darifenacin	8.9	8.9	0.1	0.9	0.1	3
Zamifenacin	7.9	7.9	0.1	1.1	0.1	3
Tolterodine	8.5	8.5	0.3	1.6	0.4	4
Oxybutynin	8.7	8.4	0.2	1.1	0.1	4

*Binding affinity estimates are taken from Eglen *et al.* (1997) with the exception of AQ-RA 741 which is taken from Dörje *et al.* (1991), and oxybutynin which is unpublished data provided by D.N. Loury and D.W. Bonhaus where $n=6$ (Roche Bioscience, Palo Alto). n =number of individual experiments each performed in triplicate.

Table 2 Antagonist affinity estimates derived from InsPs studies compared with Tris-Krebs binding data at muscarinic M₅ receptors

Antagonist	*pK _i	pK _B	s.e.mean	Hill slope	s.e.mean	n
Atropine	9.1	8.7	0.1	1.0	0.2	3
Pirenzepine	6.9	6.4	0.1	1.0	0.2	4
Methoctramine	6.4	6.3	0.2	1.0	0.1	3
AQ-RA 741	6.1	6.1	0.2	0.8	0.2	4
Himbacine	6.1	6.3	0.2	0.8	0.2	4
4-DAMP	8.9	8.6	0.2	1.2	0.3	4
p-F-HHSiD	6.7	6.6	0.1	1.4	0.4	3
Darifenacin	8.1	7.7	0.1	0.9	0.2	3
Zamifenacin	7.4	7.6	0.1	1.2	0.1	3
Tolterodine	8.6	8.6	0.2	0.9	0.1	3
Oxybutynin	7.6	6.6	0.1	0.9	0.1	3

*Binding affinity estimates are taken from Eglen *et al.* (1997) with the exception of AQ-RA 741 which is taken from Dörje *et al.* (1991), and oxybutynin which is unpublished data provided by D.N. Loury and D.W. Bonhaus where $n=6$ (Roche Bioscience, Palo Alto). n =number of individual experiments each performed in triplicate.

therefore, provided appropriate conditions for evaluating antagonist affinity estimates.

Carbachol produced a 6.5 ± 0.4 fold stimulation of inositol phosphates accumulation with a potency (pEC_{50}) of 5.9 ± 0.1 in cells expressing muscarinic M₃ receptors (mean \pm s.e.mean of 11 experiments performed in triplicate). In cells expressing muscarinic M₅ receptor, carbachol produced a 2.9 ± 0.2 fold stimulation of inositol phosphates accumulation, with a potency (pEC_{50}) of 4.8 ± 0.1 (mean \pm s.e.mean of 13 experiments performed in triplicate). No carbachol-stimulated accumulation of inositol phosphates was detected in untransfected CHO-K1 cells (Figure 1). The CHO-K1 cells

expressed the M₃ receptor protein at a density of $6075 \text{ fmol mg}^{-1}$ protein, which was 10 fold higher than the density of M₅ receptor expression (600 fmol mg^{-1} protein).

Given the relatively low potency of carbachol in cells expressing M₅ receptors, several muscarinic agonists were evaluated in order to establish whether a more potent agonist could be identified. However, there was no difference in either the potency or the magnitude of maximal [³H]-InsPs accumulation induced by (+)-cis-dioxolane ($pEC_{50} = 5.2$), carbachol ($pEC_{50} = 4.7$), or oxotremorine M ($pEC_{50} = 4.6$). In contrast, pilocarpine produced no detectable [³H]-InsPs accumulation over the concentration range studied (1 nM – 10 mM).

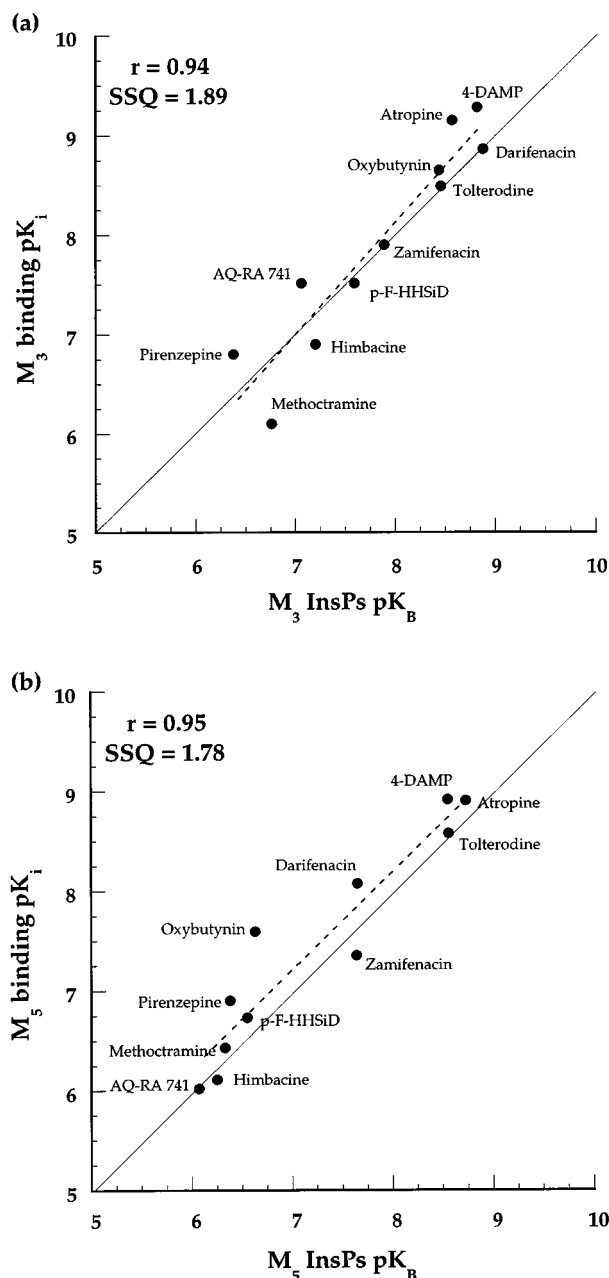


Figure 3 Correlation plots showing the relationship of binding affinity data (pK_i) generated at human recombinant muscarinic M₃ (a) and M₅ receptors (b) expressed in CHO-K1 cells with functional affinity data (pK_B) generated in the present study (see Tables 1 and 2 for source of these data). The solid line represents the line of identity, $SSQ = \sum (x - y)^2$, while the dotted line represents the correlation, where $r = \text{correlation coefficient}$.

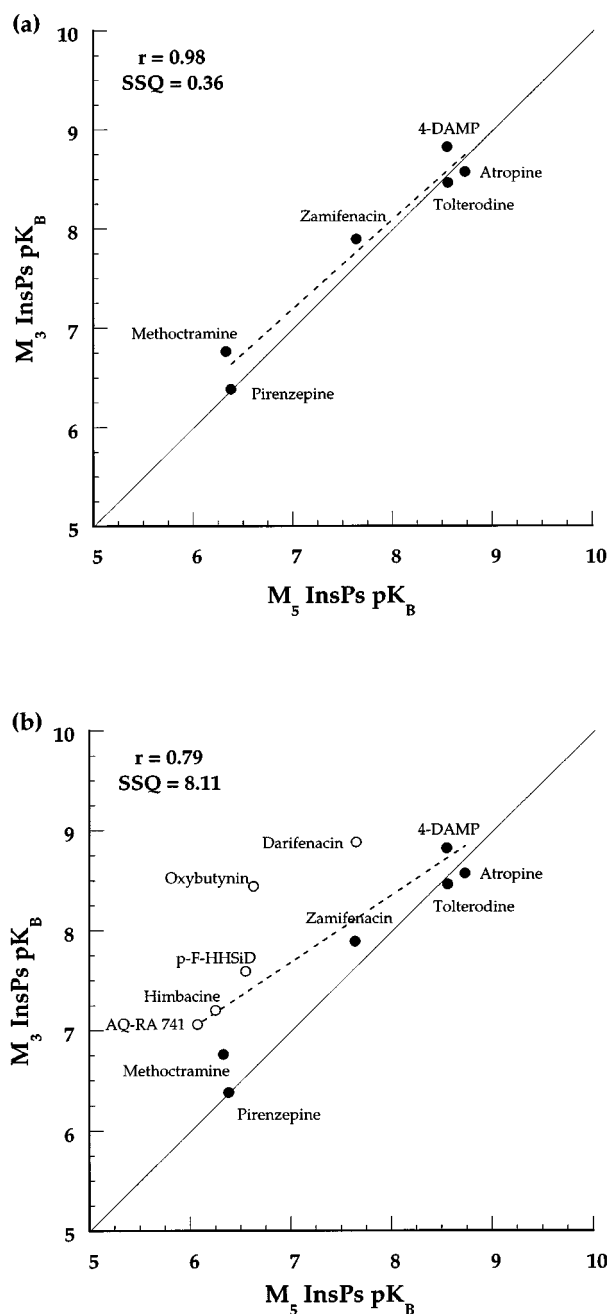


Figure 4 Correlation plots showing the relationship of functional affinity data (pK_B) of the human recombinant M₃ with the M₅ muscarinic receptor (see Tables 1 and 2 for source of these data). The solid line represents the line of identity, $SSQ = \sum (x - y)^2$, while the dotted line represents the correlation, where $r = \text{correlation coefficient}$.

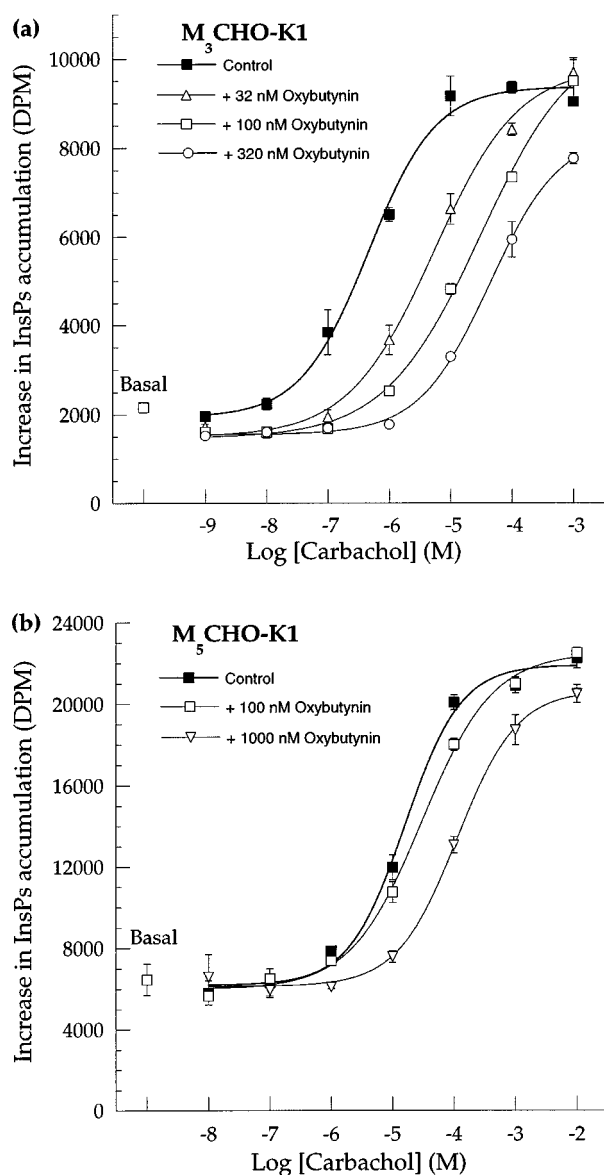


Figure 5 Inhibition of carbachol-stimulated [³H]-InsPs accumulation in CHO-K1 cells expressing human recombinant muscarinic M₃ (a) and M₅ (b) receptors. Carbachol concentration-effect curves were performed in the absence and presence of oxybutynin as indicated. Data are from representative experiments performed in triplicate. Within-experiment means and standard deviations are shown.

Antagonist-induced inhibition of carbachol-stimulated [³H]-InsPs accumulation

Concentrations of 10 μ M and 100 μ M carbachol were selected as approximately EC₉₀s against which inhibition curves to antagonists were generated in the CHO-K1 M₃ and M₅ receptor systems, respectively. All antagonists produced concentration-dependent inhibition of carbachol-stimulated [³H]-InsPs accumulation (Figure 2) from which IC₅₀ values and slopes were determined for estimation of affinities (pK_B ; see Leff & Dougall, 1993). Antagonists had no effect on basal [³H]-InsPs levels (data not shown). Tables 1 and 2 show the antagonist affinity estimates established in the present study at the M₃ and M₅ subtypes, respectively. These data were compared with those obtained previously from radioligand binding studies in similar recombinant cells.

Figure 3 shows a significant correlation between the affinity estimates previously reported from binding studies and the estimates established in the present study. (M₃: $\sum(x-y)^2 = 1.89$, $r = 0.94$, pK_i vs pK_B and M₅: $\sum(x-y)^2 = 1.78$, $r = 0.95$, pK_i vs pK_B). Figure 4 shows the correlation between the antagonist affinity estimates generated in the present study at the M₃ and M₅ receptors. This demonstrates the similarity in the antagonist affinity profile of these two subtypes but also highlights those antagonists (b), which are able to discriminate between these subtypes.

Oxybutynin-induced shifts in carbachol concentration-effect curves

In cells expressing the M₃ subtype oxybutynin produced concentration-dependent rightward shifts in the concentration-effect curves to carbachol (Figure 5a) yielding sufficient data for a Schild plot, with a slope not significantly different from unity (1.0 ± 0.1) and an antagonist affinity of 8.4 ± 0.2 ($n = 3$). In cells expressing the M₅ subtype oxybutynin also produced a rightward shift in the concentration-effect curve to carbachol, but because of the low potency of carbachol, insufficient data could be generated for Schild analysis (Figure 5b). Nevertheless, the apparent affinity estimate generated from the shift by a single concentration of oxybutynin was 6.4 ± 0.2 ($n = 3$). These values for oxybutynin at the M₃ and M₅ receptors are in good agreement with the estimates established using antagonist inhibition curves (pK_B ; see Leff & Dougall, 1993) in Tables 1 and 2, respectively.

Discussion

The present study has compared functional affinity estimates of several muscarinic antagonists at muscarinic M₃ and M₅ receptors expressed in CHO-K1 cells. These data demonstrate a good correlation between the functional affinity estimates obtained herein and binding affinity estimates previously established in these cells (Buckley *et al.*, 1989; Dörje *et al.*, 1991; Bolden *et al.*, 1992; Lazareno & Birdsall, 1993; Eglén *et al.*, 1997). These data also highlight the similarity in the pharmacology of these two receptor subtypes (Choppin *et al.*, 1998). Reeve *et al.* (1997) previously reported that AQ-RA 741 and AF-DX 384, are able to discriminate between M₃ and M₅ receptor subtypes. In the present study, we have confirmed these findings with AQ-RA 741 and in addition we have identified additional compounds, himbacine, p-F-HHSiD, darifenacin, and oxybutynin, that are also able to discriminate between muscarinic M₃ and M₅ receptors. However, all these compounds display higher affinity for the M₃ subtype and as yet no compound has been identified which can discriminate between M₃ and M₅ receptors by displaying a higher affinity at the M₅ receptor subtype.

Agonist studies

In the present study, an initial determination of the functional antagonist affinity estimates was carried out in the CHO-K1 M₃ cells by performing shifts of the carbachol-stimulated [³H]-InsPs accumulation using three different concentrations of antagonists. This enabled Schild analysis to be performed and a pA_2 value to be determined for each antagonist (Arunlakshana & Schild, 1959). However, when the response to carbachol was evaluated in the CHO-K1 M₅ receptor system the potency was 10 fold lower, (4.8 ± 0.1 versus 5.9 ± 0.1) such that shifts to only a single antagonist concentration could be

achieved. The reasons for the difference in carbachol potency may reflect differences in the density of receptor protein, which was 10 fold greater in the CHO-K1 M₃ system as compared to the M₅ system. The potencies of other muscarinic agonists were evaluated in the CHO-K1 M₅ system in an effort to identify a more potent agonist, which might enable Schild analysis to be performed in the CHO-K1 M₅ cell system. However, there was little difference in the potency or the magnitude of maximal [³H]-InsPs accumulation induced by (+)-cis-dioxolane, carbachol or oxotremorine M, and pilocarpine was unable to stimulate [³H]-InsPs accumulation. Therefore, since it was not technically feasible to generate curve shifts with multiple concentrations of antagonist in the CHO-K1 M₅ system, an alternative approach was used. A concentration of carbachol was selected which caused approximately 90% of the maximum [³H]-InsPs accumulation (100 μ M) and antagonist-inhibition curves were performed which enabled an affinity estimate to be generated based on the Leff & Dougall (1993) derivation of the Cheng-Prusoff equation. The experiments in the CHO-K1 M₃ receptor system were then repeated using the same approach, in order to facilitate comparison between these two cell systems. There was, however, good agreement between antagonist affinities established in the CHO-K1 M₃ receptor systems using Schild analysis and those established using the method of Leff & Dougall (1993). Given the difference between binding and functional affinity estimates for oxybutynin in these studies at the CHO-K1 M₅ receptor system, both the Schild and Leff-Dougall approaches were used with oxybutynin to corroborate the lower than expected affinity estimate obtained.

Antagonist studies

The antagonist apparent affinity estimates obtained in the present study compare well with binding affinity estimates, with two notable exceptions. Atropine appeared to be approximately 10 fold less potent at M₃ receptors and oxybutynin was approximately 10 fold less potent at the M₅ receptor, compared to the binding affinity estimates for these two antagonists. The low affinity of atropine might be explained by endogenous atropine esterase activity associated with the CHO-K1 system, however, a series of experiments performed in the presence of methyl butyrate (100 μ M to inhibit atropine esterase activity), failed to improve the affinity estimate of atropine (data not shown). Given that the binding affinity estimates were obtained in membrane preparations at 20°C and the functional affinity estimates obtained in whole cells at 37°C it is perhaps not surprising to observe some differences. However, the correlation between functional and binding affinity estimates was in general very good as reflected by the correlation plots.

It is unclear why oxybutynin displayed lower affinity for muscarinic M₅ receptors in the present study than that predicted by binding studies. However, the increased M₃ over M₅ receptor selectivity resulting from these data may relate to the >10 fold disparity between the muscarinic M₃ and M₅ receptor densities in the CHO-K1 cell clones. Interpretation of these data would be strengthened if antagonist affinities were established at these receptor subtypes when expressed at similar densities, however, these studies were not undertaken. Therefore, while the implication from the current finding, using InsPs derived affinity estimates, is an improved discrimination of oxybutynin, between muscarinic M₃ and M₅ receptors, the utility of oxybutynin as a discriminator between M₃ and M₅ receptors should be confirmed in cell systems where receptor expression levels are comparable. This

could be achieved using alternative clonal cell lines with similar expression levels or receptor alkylation techniques could be undertaken to reduce the number of M₃ receptors to a level comparable to the M₅ CHO-K1 system.

The present study highlights the need for a range of antagonists to be used in the characterization of muscarinic receptor subtypes in order that an unambiguous characterization may be achieved. Characterization of a new receptor subtype is often performed using a very simplistic approach. The non-selective antagonist atropine is included, to determine the muscarinic nature of the receptor, and then a single antagonist selective for M₁, M₂ and M₃ receptor subtypes (e.g.: pirenzepine – M₁ selective, methoctramine – M₂ selective and 4-DAMP – M₃ selective antagonist) are included. As is evident from Figure 4a such a characterization would not adequately discriminate between M₃ and M₅ receptors. Figure 4b identifies the compounds that would improve the characterization and enable discrimination between these two subtypes. Reervers *et al.* (1997), have previously reported that AQ-RA 741 shows some 10 fold lower affinity for M₅ receptors than for the M₃ subtype, an observation which is confirmed by the present study. In addition, however, the present study identifies himbacine as having lower affinity for the M₅ subtype than for the M₃ subtype. Darifenacin and p-F-HHSiD, both M₃ selective antagonists, provide advantages over the other M₃ antagonists, 4-DAMP and zamifenacin, in that they have lower affinity at the M₅ receptor subtype. Additionally, oxybutynin with lower affinity at the M₅ subtype compared to the M₃, provides additional separation. However, no compound was identified in the present study as having higher affinity for the M₅ subtype over the M₃ subtype and clearly such a compound would be a most useful tool.

Implications for receptor characterization

These observations raise questions with regard to responses reportedly mediated by muscarinic M₃ receptors, particularly when the characterization was based on a limited number of antagonists of limited selectivity. In particular ocular tissues, such as iris and ciliary smooth muscle appear to be candidates for a peripheral M₅ receptor mediated response. Thus, immunoprecipitation studies in human iris-ciliary body identified the presence of M₅ as well as M₃ receptors (Gil *et al.*, 1997). Bognar *et al.* (1989; 1992) performed an extensive characterization of the muscarinic receptor mediating contractions of the rabbit iris sphincter. These authors reported the presence of a muscarinic receptor with an M₃-like pharmacology, but which displayed low affinity for p-F-HHSiD and secoverine, suggesting the possibility of an M₅ subtype. However, recent studies in rabbit iris sphincter muscle from our group (Choppin *et al.*, 1998) have not confirmed the low affinity of p-F-HHSiD and secoverine in this preparation. Consequently it was concluded that these data are more consistent with M₃ receptors mediating contraction of this tissue. Although most evidence to date suggests M₅ receptors are confined to the CNS, there is evidence that they may be found on blood cells, specifically, microglial/macrophage cells express mRNA for the M₅ receptor subtype (Ferrari-DiLeo & Flynn, 1995). However, these transcripts were associated with brain tissue and it is unclear as to whether peripheral/circulating macrophages also express the M₅ receptor subtype. Circulating lymphocytes possess muscarinic receptors, but the subtype(s) has not yet been identified (Zalcman *et al.*, 1981).

The recent generation of gene-targeted mice, lacking the M₅ receptor, has begun to shed light on the role of this receptor subtype (Yeomans *et al.*, 1998). However, the development of

M₅ selective ligands and antibodies remains an important requirement for the identification of tissues and/or cell lines that express the native M₅ receptor protein. The present study has identified a number of muscarinic antagonists that, while lacking selectivity for the M₅ receptor subtype, should provide useful tools for separating M₅ receptors from M₃ receptors, because of their low affinity for the M₅ receptor subtype. High affinity M₅ selective ligands are currently not available. Nevertheless, through a combination of classical pharmacology, using those compounds that discriminate M₃ and M₅

receptors, and molecular biological techniques that demonstrate the presence of message or protein for the M₅ receptor subtype, it should be possible to identify a functional role for endogenous M₅ receptors.

The authors would like to thank Joel Gever and Trena Meloy for their valuable technical support, and the Department of Molecular Pharmacology for providing the CHO-K1, M₃ and M₅ receptor systems. The contributions of Dana Loury and Doug Bonhaus (oxybutynin binding affinity data) are also gratefully acknowledged.

References

- ARUNLAKSHANA, O. & SCHILD, H.O. (1959). Some quantitative uses of drug antagonists. *Br. J. Pharmacol. Chemother.*, **14**, 48–58.
- BOGNAR, I.T., ALTES, U., BEINHAEUER, C., KESSLER, I. & FUDER, H. (1992). A muscarinic receptor different from the M₁, M₂, M₃ and M₄ subtype mediates the contraction of the rabbit iris sphincter. *Naunyn-Schmiedeberg's Arch. Pharmacol.*, **345**, 611–618.
- BOGNAR, I.T., BAUMANN, B., DAMMANN, F., KNÖLL, B., MEINCKE, M. & FUDER, H. (1989). M₂ muscarinic receptors on the iris sphincter muscle differ from those on iris noradrenergic nerves. *Eur. J. Pharmacol.*, **163**, 263–274.
- BOLDEN, C., CUSACK, B. & RICHELSON, E. (1992). Antagonism by antimuscarinic and neuroleptic compounds at the five cloned human muscarinic cholinergic receptors expressed in chinese hamster ovary cells. *J. Pharmacol. Exp. Ther.*, **260**, 576–580.
- BROWN, E., KENDALL, D.A. & NAHORSKI, S.R. (1984). Inositol phospholipid hydrolysis in rat cerebral cortical slices. I. Receptor characterization. *J. Neurochem.*, **42**, 1379–1387.
- BUCKLEY, N.J., BONNER, T.I., BUCKLEY, C.M. & BRANN, M.R. (1989). Antagonist binding properties of five cloned muscarinic receptors expressed in CHO-K1 cells. *Mol. Pharmacol.*, **35**, 469–476.
- CAULFIELD, M.P. & BIRDSALL, N.J.M. (1998). International Union of Pharmacology. XVII. Classification of muscarinic acetylcholine receptors. *Pharmacol. Rev.*, **50**, 279–290.
- CHENG, Y.C. & PRUSOFF, W.H. (1973). Relationship between inhibition constant (K_i) and the concentration of inhibitor which causes 50% inhibition (IC₅₀) of an enzymatic reaction. *Biochem. Pharmacol.*, **22**, 3099–3108.
- CHOPPIN, A., EGLIN, R.M. & HEGDE, S.S. (1998). Pharmacological characterization of muscarinic receptors in rabbit isolated iris sphincter muscle and urinary bladder smooth muscle. *Br. J. Pharmacol.*, **124**, 883–888.
- DÖRJE, F., WESS, J., LAMBRECHT, G., TACKE, R., MUTSCHLER, E. & BRANN, M.R. (1991). Antagonist binding profiles of five cloned human muscarinic receptor subtypes. *J. Pharmacol. Exp. Ther.*, **256**, 727–733.
- EGLIN, R.M., BONHAUS, D.W., CALIXTO, J.J., CHOPPIN, A., LEUNG, E., LOEB, M., LOURY, D., MOY, T., WILDA, M. & HEGDE, S.S. (1997). Characterization of the interaction of tolterodine at muscarinic receptor subtypes in vitro and in vivo. *Br. J. Pharmacol.*, **120**, 63P.
- FERRARO-DILEO, G. & FLYNN, D.D. (1995). Characterization of muscarinic receptors on cultured microglial cells. *Life Sci.*, **56**, 1037 (abstract).
- GIL, D.W., KRAUSS, H.A., BOGARDUS, A.M. & WOLDEMUSSE, E. (1997). Muscarinic receptor subtypes in human iris-ciliary body measurement by immunoprecipitation. *Inv. Ophthalmol. Vis. Sci.*, **38**, 1434–1442.
- LAZARENO, S. & BIRDSALL, N.J.M. (1993). Pharmacological characterization of acetylcholine-stimulated [³⁵S]-GTPγS binding mediated by human muscarinic m1-m4 receptors: antagonist studies. *Br. J. Pharmacol.*, **109**, 1120–1127.
- LEFF, P. & DOUGALL, I.G. (1993). Further concerns over Cheng-Prusoff analysis. *Trends Pharmacol. Sci.*, **15**, 141–144.
- REEVER, C.M., FERRARI-DILEO, G. & FLYNN, D.D. (1997). The M₅ (m5) receptor subtype: Fact or fiction? *Life Sci.*, **60**, 1105–1112.
- WATSON, N., DANIELS, D.V., FORD, A.P.D.W., EGLIN, R.M. & HEGDE, S.S. (1998). Comparative pharmacology of human muscarinic m3 and m5 cholinergic receptors expressed in chinese hamster ovary (CHO) cells. *Br. J. Pharmacol.*, **123**, 268P.
- YEOMANS, J., TAKEUCHI, J., JIA, Z., FULTON, J., ABRAMOV-NEWERLY, W., JAMOT, L. & RÖDER, J. (1998). Gene-targeted mice lacking M₅ receptors: Genotypes and Behaviour. *Life Sci.*, abstract (in press).
- ZALCMAN, S.J., NECKERS, L.M., KAAYALP, O. & WYATT, R.J. (1981). Muscarinic cholinergic binding sites on intact human lymphocytes. *Life Sci.*, **29**, 69–73.

(Received December 15, 1998)

Revised February 11, 1999

Accepted February 18, 1999